Research Square

Preprints are preliminary reports that have not undergone peer review.
They should not be considered conclusive, used to inform clinical practice,
or referenced by the media as validated information.

Geometry-Aware Depth Anomaly Detection and Adaptive Decision Modeling for Automated Robotic Quality Sorting

Shahriar Tasnim

shahriart0013@gmail.com

Lamar University https://orcid.org/0009-0004-6093-9615

Research Article

Keywords: Industrial 3D Anomaly Detection, Geometric Feature Fusion, Depth-Based Inspection, Surface Defect Localization, Shape Descriptors, Uncertainty Estimation, Adaptive Robotic Sorting

Posted Date: November 13th, 2026

DOI: https://doi.org/10.21203/rs.3.rs-11703978/v1

License: This work is licensed under a Creative Commons Attribution 4.0 International License.
Read Full License

Additional Declarations: The authors declare no competing interests.

Geometry-Aware Depth Anomaly Detection and Adaptive Decision Modeling for Automated Robotic Quality Sorting

Shahriar Tasnim
Email: shahriart0013@gmail.com
Master of Engineering Science in Electrical & Computer Engineering
Lamar University, Beaumont, Texas, USA
ORCiD: https://orcid.org/0009-0004-6093-9615

Abstract
Industrial 3D anomaly detection remains challenging when defective surface structures must be distinguished from normal geometric variations across different industrial components. This study presents a geometry-aware anomaly detection framework that integrates local surface characteristics with global object-shape descriptors for industrial defect identification and localization. The proposed framework is evaluated using the MVTec 3D-AD benchmark, comprising 4,147 industrial 3D scans across ten object categories. Local geometric characteristics, including surface normals, curvature, depth variation, and neighborhood consistency, are combined with global descriptors, including convexity, solidity, and void ratio, to construct a complementary geometric representation. The experimental evaluation examines conventional geometric thresholding, an unsupervised 3D anomaly detection baseline, and the proposed local–global feature-fusion approach. Image-level anomaly detection and pixel-level defect localization are assessed using AUROC, average precision, Intersection over Union, and Dice similarity. Feature-ablation analysis investigates the respective contributions of local and global geometric representations. Furthermore, anomaly severity and prediction uncertainty are incorporated into a three-action quality-inspection strategy comprising acceptance, rejection, and additional inspection. The sorting component is evaluated through a cost-sensitive simulation that considers false acceptance, false rejection, and additional-inspection requirements. The study connects geometric anomaly detection with uncertainty-aware quality control decision modeling and investigates the contribution of complementary geometric information to automated industrial inspection. Physical robotic deployment and validation under actual manufacturing conditions remain outside the scope of this experimental evaluation.

Keywords: Industrial 3D Anomaly Detection, Geometric Feature Fusion, Depth-Based Inspection, Surface Defect Localization, Shape Descriptors, Uncertainty Estimation, Adaptive Robotic Sorting.

I. Introduction
Industrial quality inspection increasingly relies on three-dimensional sensing to identify structural defects that may not be clearly represented in conventional two-dimensional images. Depth information provides geometric measurements of component surfaces, allowing localized deformation, surface irregularities, and structural inconsistencies to be examined. However, accurate anomaly detection remains challenging when industrial components exhibit different shapes, surface structures, and natural geometric variations. This study investigates a geometry-aware anomaly detection framework that combines local surface features with global shape characteristics and translates predicted defect severity into uncertainty-aware quality sorting decisions using the MVTec 3D-AD benchmark.

A. Background and Motivation
Three dimensional anomaly detection has become an important research area in automated industrial inspection. Unlike conventional appearance-based inspection, depth-based analysis provides spatial information about component geometry. Surface normals, curvature, and depth variation can represent localized structural changes, while convexity, solidity, and void ratio describe broader object characteristics. These features provide complementary information for identifying defects across different industrial components. The MVTec 3D-AD dataset provides an appropriate benchmark for investigating these characteristics through ten industrial object categories and annotated anomalous observations. Nevertheless, variations in object geometry can complicate anomaly identification. A local surface deviation may represent a genuine defect in one component but normal structural variation in another. This motivates the

integration of local geometric measurements with global shape descriptors. Furthermore, industrial inspection decisions require more than anomaly classification because uncertain predictions may lead to incorrect acceptance, unnecessary rejection, or additional inspection.

B. Problem Statement

Conventional depth-based anomaly detection methods often rely on localized geometric deviations or predefined thresholds to identify defective surface regions. However, local geometric measurements alone may not adequately distinguish genuine defects from normal structural variations across different industrial components. A localized surface irregularity may indicate a defect without substantially changing the overall object geometry, whereas naturally occurring geometric variations may produce deviations that resemble defective structures. Global shape descriptors provide complementary structural information but may fail to identify small localized abnormalities when used independently. Therefore, the central problem addressed in this study is the limited integration of local surface geometry and global object-shape characteristics within a unified 3D anomaly detection framework. In addition, anomaly detection accuracy alone does not establish whether an inspection decision is appropriate when model predictions are uncertain. A further challenge is connecting anomaly severity and prediction uncertainty with acceptance, rejection, and additional-inspection decisions. This study addresses these interconnected problems through geometry-aware feature fusion, spatial anomaly localization, and uncertainty-aware simulated quality sorting using the MVTec 3D-AD benchmark.

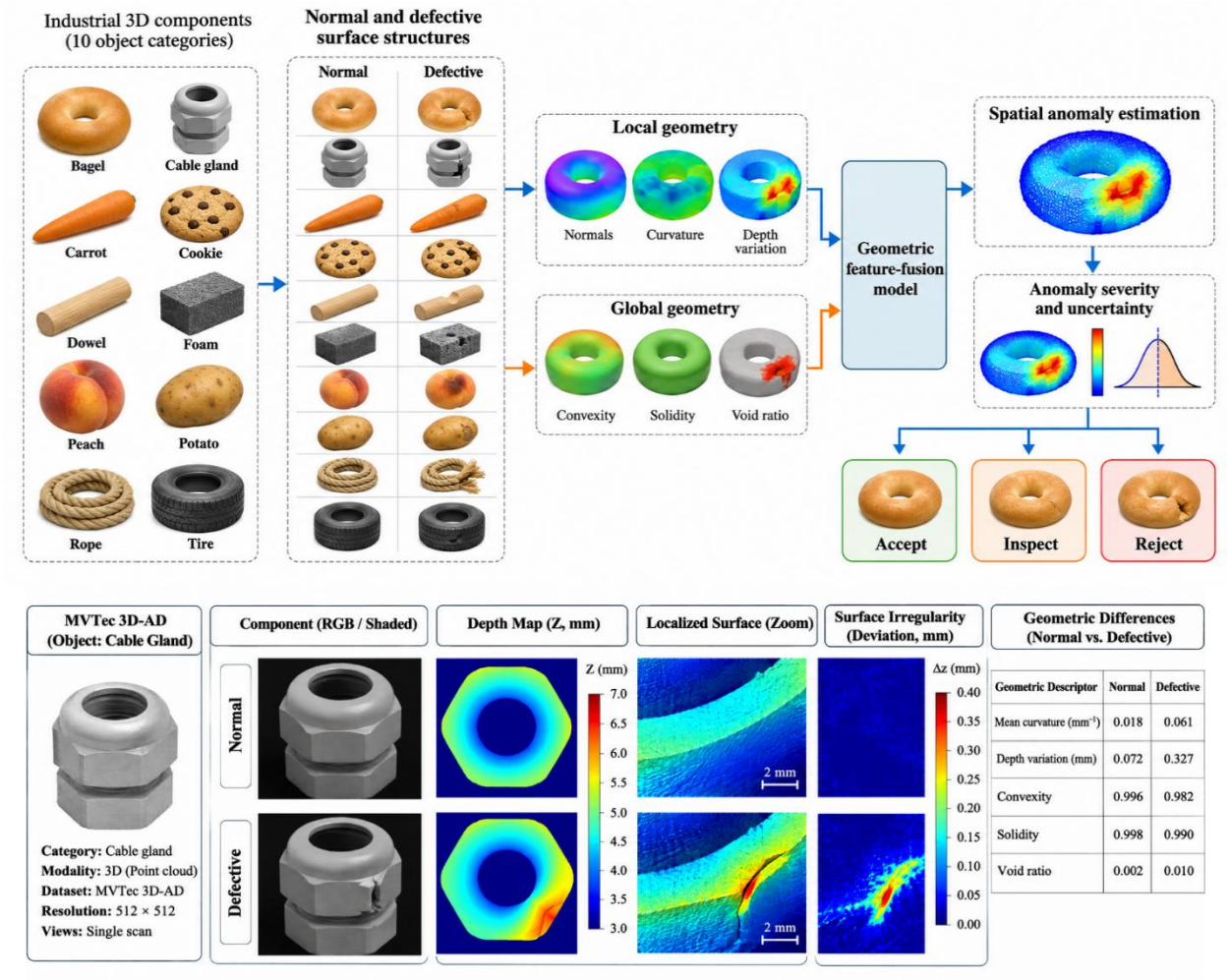


Fig. 1. Problem Representation and Proposed Research Framework.

C. Proposed Solution

This study proposes a geometry-aware anomaly detection framework that integrates local surface characteristics with global object-shape descriptors to identify and localize industrial geometric defects. The local geometric representation incorporates surface normals, curvature, depth variation, and neighborhood consistency to capture localized structural

irregularities. The global representation incorporates convexity, solidity, and void ratio to characterize broader object geometry. These complementary representations are integrated through a local–global feature-fusion model to generate spatial anomaly scores and object-level anomaly assessments. The framework further incorporates anomaly severity and prediction uncertainty into a three-action quality-inspection strategy involving acceptance, rejection, and additional inspection. The experimental evaluation uses the MVTec 3D-AD benchmark and examines geometric feature representation, comparative anomaly detection, pixel-level defect localization, feature contributions, and cost-sensitive simulated sorting. The sorting component represents a simulated inspection decision process rather than a physically deployed robotic system.

D. Contributions

This study makes methodological and experimental contributions to geometry-aware industrial 3D anomaly detection. First, it develops a complementary geometric representation that integrates local surface characteristics, including surface normals, curvature, depth variation, and neighborhood consistency, with global shape descriptors, including convexity, solidity, and void ratio. Second, it formulates a local–global feature-fusion approach for generating spatial anomaly predictions and object-level defect assessments. Third, it examines the contribution of local and global geometric feature groups through comparative and ablation evaluations of anomaly detection and defect localization. Fourth, it connects anomaly severity and prediction uncertainty with a cost-sensitive three-action quality-inspection strategy involving acceptance, rejection, and additional inspection. Finally, the framework is evaluated using the MVTec 3D-AD benchmark through image-level detection, pixel-level localization, geometric feature analysis, and simulated sorting. The contributions are limited to the implemented experimental evaluation and do not imply physical robotic deployment or industrial production validation.

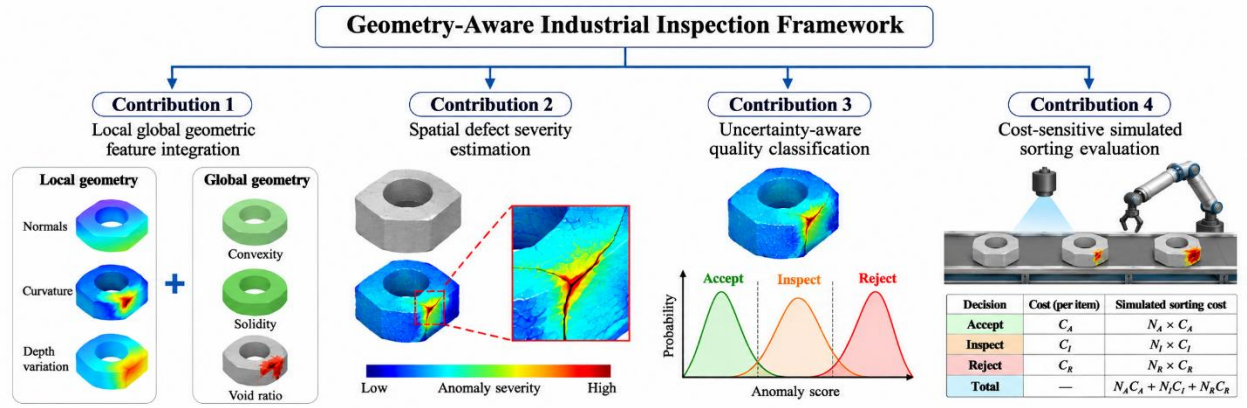


Fig. 2. Principal Research Contributions.

E. Paper Organization

The remainder of this paper is organized as follows. Section II reviews related research on industrial 3D anomaly detection, geometric feature extraction, feature fusion, and defect localization. Section III describes the research methodology, including dataset preparation, geometric feature extraction, baseline models, the proposed local–global feature-fusion architecture, anomaly severity estimation, uncertainty analysis, and simulated quality sorting. Section IV presents the experimental results and discussion, covering dataset characteristics, geometric feature representation, comparative anomaly detection, defect localization, uncertainty-aware sorting, and the limitations of the proposed framework. Section V concludes the study by summarizing its principal methodological and experimental contributions and identifying directions for future research.

II. Related Work

This section reviews existing research on industrial 3D anomaly detection, geometric feature extraction, and automated defect localization. It also examines the limitations of existing approaches and identifies the research gaps addressed by the proposed framework.

A. Industrial 3D Anomaly Detection

Industrial anomaly detection has traditionally relied on visual inspection and image-based classification. The introduction of MVTec 3D-AD provided a benchmark for unsupervised detection and localization of geometric defects using high-resolution 3D scans and ground-truth annotations [1]. Subsequent research

introduced deep geometric descriptors and student teacher learning to identify abnormal structures in point clouds using defect-free training observations [2]. These developments demonstrated the importance of spatial geometric information in industrial inspection.

B. Geometric Feature Extraction and Surface Defect Detection

Geometric feature extraction provides information about surface orientation, curvature, and structural irregularities. Surface-normal-based filtering has been investigated for identifying defects in 3D point-cloud measurements [3]. Point-cloud density variations have also been addressed through density-aware up sampling, which improves geometric representation across regions with different sampling densities [4]. Other research has investigated visual-to-geometric feature reconstruction to improve the representation of industrial anomalies through complementary feature information [5].

C. Feature Fusion and Advanced Anomaly Detection

Recent studies have investigated feature integration and specialized learning architectures for 3D industrial anomaly detection. Hybrid geometric filtering methods have been examined for surface-defect classification using point-cloud information [6]. Uni-3DAD introduced a GAN-inversion-based approach for anomaly detection on model-free products [7]. Geometric-prior-based detection further investigated surface-normal information and geometric feature fusion for identifying structural abnormalities [8]. Importance-aware ensemble learning has also been explored to combine complementary model predictions for 3D point-cloud anomaly detection [9].

D. Research Gaps

Despite recent developments in industrial 3D anomaly detection, several limitations remain relevant to geometry-aware defect inspection. First, local surface measurements and global object-shape descriptors are frequently considered as separate sources of geometric information. Their integration is important because localized defects and broader structural variations may exhibit different geometric characteristics. Second, anomaly detection performance does not necessarily establish the quality of spatial defect localization. Evaluating the contributions of local and global feature groups through comparative and ablation experiments is therefore necessary to understand their respective roles in identifying and locating geometric abnormalities. Third, conventional anomaly classification generally focuses on distinguishing normal and defective observations without explicitly considering the consequences of uncertain predictions for subsequent inspection decisions. The relationship between anomaly severity, prediction uncertainty, and cost-sensitive quality sorting consequently requires further investigation. To address these limitations, this study develops a geometry-aware local–global feature-fusion framework and evaluates its detection, localization, feature contributions, and uncertainty-aware simulated sorting performance using the MVTec 3D-AD benchmark.

III. Methodology

The methodology is organized into a sequential experimental workflow covering 3D dataset preparation, geometric feature extraction, baseline evaluation, feature-fusion anomaly modeling, and uncertainty-aware quality sorting. The framework uses depth-derived surface information and global object geometry to generate spatial defect predictions, which are subsequently evaluated through a simulated industrial inspection and sorting process.

A. Research Design

The methodology establishes an experimental framework for evaluating geometry-aware anomaly detection and uncertainty-aware quality sorting using the MVTec 3D-AD benchmark. The research process consists of dataset acquisition and preparation, local and global geometric feature extraction, baseline anomaly detection, local–global feature fusion, anomaly severity and uncertainty estimation, and simulated sorting evaluation. The local geometric representation captures surface-level irregularities through surface normals, curvature, depth variation, and neighborhood consistency. The global representation describes broader object geometry through convexity, solidity, and void ratio. The extracted representations are integrated to generate spatial anomaly predictions and object-level assessments. Finally, the predicted anomaly severity and uncertainty are used to examine acceptance, rejection, and additional-inspection decisions through a simulated cost-sensitive quality-control process. The experimental evaluation is based on the original dataset partitions, and no physical robotic deployment is claimed.

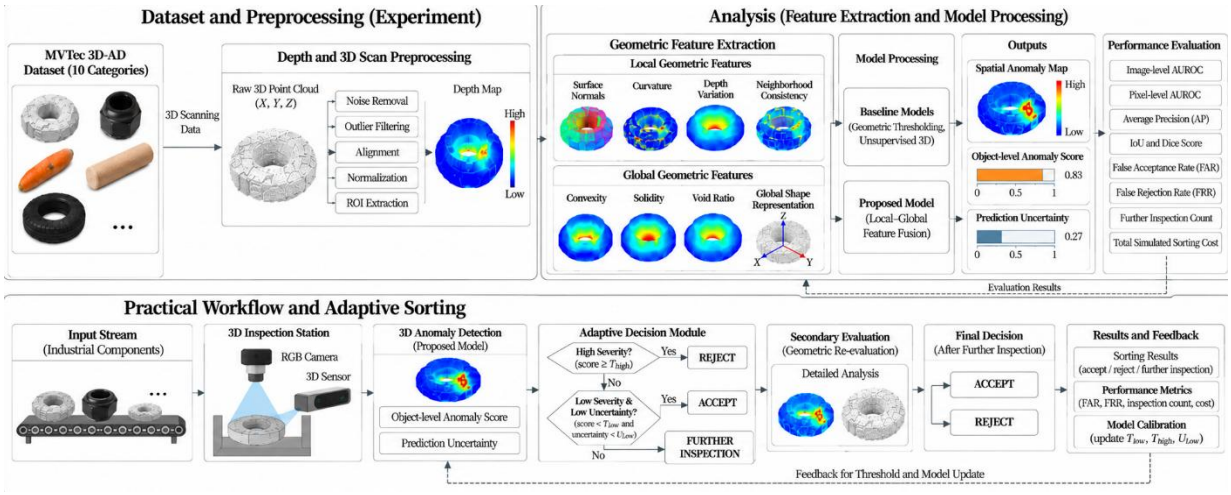


Fig. 3. Overall Experimental Research Workflow.

B. Dataset Acquisition and Experimental Data Preparation

The MVTec 3D-AD dataset is used as the primary experimental benchmark for evaluating the proposed geometry-aware anomaly detection framework. It comprises 4,147 industrial 3D scans distributed across ten object categories. The dataset provides defect-free training and validation observations and annotated normal and anomalous test observations. The original dataset partitions are preserved throughout the experimental process. Dataset preparation includes structural verification, depth-map inspection, invalid-measurement identification, spatial normalization where required, and geometric feature preparation. The processed observations retain their original sample identifiers and category information to maintain correspondence with the benchmark annotations. The training partition establishes the normal geometric reference representation, the validation partition supports model configuration and threshold selection, and the test partition is reserved for final detection, localization, and simulated sorting evaluation. The category-wise sample distribution is presented in Table II, while defect types and annotation characteristics are summarized in Table III.

i. Dataset Selection and Characteristics

The MVTec 3D Anomaly Detection (MVTec 3D-AD) dataset is selected as the primary benchmark for evaluating the proposed geometry-aware anomaly detection framework. The dataset contains 4,147 industrial 3D scans distributed across ten object categories. The original dataset partitions are preserved to maintain the benchmark evaluation protocol. Defect-free training observations are used to establish the reference geometric representation and develop the anomaly detection model. The validation partition is used for model configuration and decision-threshold selection, where applicable. The test partition is reserved for final evaluation using the available anomaly annotations. The category-wise sample distribution and defect characteristics are reported in Section IV-A.

ii. Data Acquisition and Structural Verification

A structural verification procedure checks the availability of the expected object categories, scan files, training and validation partitions, anomalous test samples, and corresponding annotation files. Each scan is inspected for missing values, invalid depth measurements, incomplete spatial coordinates, and inconsistencies in the recorded data dimensions. Samples with invalid measurements are identified before feature extraction. The preprocessing procedure distinguishes missing or invalid measurements from genuine surface depressions because removing actual geometric defects would distort the anomaly distribution. The original sample identifiers are preserved throughout processing. A metadata index associates each observation with its object category, partition, scan identifier, valid-point count, and annotation availability. This index supports reproducibility, category-level evaluation, and the identification of inconsistencies between the original data and processed observations.

iii. Depth Representation and Geometric Data Preparation

The acquired 3D observations are represented using their available spatial coordinates and depth information. For each valid point, the spatial representation describes its position relative to the object coordinate system. The depth component provides the principal measurement for examining local surface displacement and geometric deviations. Invalid measurements are excluded from neighborhood

calculations, while valid observations are retained for subsequent geometric analysis. Where necessary, point-cloud normalization is applied to reduce differences in coordinate scale and orientation. Normalization parameters are derived without using anomaly labels, preventing information leakage into the unsupervised training process. Local neighborhoods are constructed around individual surface points using spatial proximity. Neighborhood size is treated as a model parameter because small neighborhoods capture localized surface disturbances, whereas larger neighborhoods represent broader geometric structures. The same neighborhood-generation procedure is applied consistently across training, validation, and test observations.

iv. Experimental Data Partitioning

The original dataset partitions are preserved rather than randomly redistributing individual scans. This decision prevents anomalous test observations from entering the training process and maintains comparability with the benchmark's intended unsupervised evaluation setting. The normal training partition is used to calculate geometric reference statistics and fit the anomaly detection components. The defect-free validation partition is used to examine score distributions, calibrate uncertainty estimates, and select decision thresholds. The anomalous test partition is reserved for final evaluation against the available ground-truth annotations. The validation process does not use test labels for parameter selection. All feature normalization parameters, model parameters, and decision thresholds are fixed before final test evaluation. Category-specific performance is reported alongside aggregate results to account for variations in object shape and surface structure.

C. Geometric Feature Extraction and Representation

The proposed geometric representation consists of local surface features and global object-shape descriptors. The local feature group includes surface normals, local curvature, depth variation, and neighborhood consistency. These features characterize surface orientation, localized bending, depth displacement, and structural differences between neighboring points. The global feature group includes convexity, solidity, and void ratio, which represent broader geometric properties of industrial components. Shape consistency is included only where supported by the implemented feature extraction procedure. The two feature groups provide complementary geometric information for the proposed local–global feature-fusion architecture. Their analytical roles are summarized in Table I, and their visual representation is presented in Figures 6 and 7.

i. Local Surface Normal Estimation

Surface normals are calculated to represent the orientation of individual surface regions. For each valid 3D point, neighboring points are identified within the selected spatial neighborhood. A local covariance representation is then constructed from the neighboring coordinates, and the eigenvector associated with the smallest eigenvalue is used as the estimated surface-normal direction. The normal representation captures changes in surface orientation that may arise from scratches, dents, deformations, missing material, and other structural irregularities. The angular relationship between neighboring normal vectors is examined to identify abrupt orientation changes. Consistent surface regions generally exhibit relatively stable normal directions, whereas defective regions may produce localized orientation discontinuities. Normal estimation is performed using the same neighborhood configuration across the experimental partitions. This prevents differences in feature computation from affecting comparisons between normal and anomalous observations.

ii. Local Curvature and Surface Irregularity

Local curvature is extracted to characterize surface bending and geometric variation. The eigenvalue distribution of each neighborhood provides information about the local surface structure. The resulting curvature descriptors distinguish relatively flat regions from areas exhibiting pronounced geometric changes. Surface irregularity is further examined through neighboring-point displacement and local depth variation. These measurements provide complementary information because two surface regions may have similar average depth but substantially different local geometric structures. The extracted features are evaluated for sensitivity to localized defects and variations in object shape. Their individual distributions are examined across the ten object categories to identify features that provide useful separation between normal surface structures and anomalous regions.

iii. Global Shape Descriptors

Global shape descriptors characterize the overall geometric structure of each industrial component. Unlike local surface features, which represent small spatial neighborhoods, global descriptors capture object-level properties that remain informative across larger surface regions. Convexity is calculated to examine the relationship between the object's observed surface and its convex geometric envelope. Solidity represents the proportion of the enclosing volume

occupied by the observed object geometry. Void ratio characterizes the relative presence of internal or unoccupied spatial regions within the selected geometric representation. These descriptors are included because the user's earlier thesis work involved void ratio, convexity, and solidity. Their incorporation provides continuity between the previous geometric analysis and the present 3D anomaly detection investigation. However, these descriptors are treated as complementary indicators rather than direct defect labels. Their suitability is examined through category-level feature analysis and validation performance.

iv. Geometric Feature Normalization

The extracted features have different numerical ranges and distributions. Surface curvature, depth variation, normal deviation, and global shape descriptors therefore require consistent scaling before feature fusion. Feature normalization parameters are estimated from the normal training observations. The same parameters are subsequently applied to validation and test samples. This procedure prevents test-set information from influencing the geometric representation. The normalized feature set is organized into two principal groups: local geometric features and global shape features. The local group contains surface normals, curvature, neighboring-point depth differences, and local geometric consistency. The global group contains convexity, solidity, void ratio, and object-level shape characteristics.

D. Baseline Anomaly Detection Models

The baseline anomaly detection models establish reference performance for evaluating the proposed geometry-aware feature-fusion approach. The comparative evaluation includes conventional geometric thresholding and an existing unsupervised 3D anomaly detection baseline. These methods are assessed alongside the proposed local–global feature-fusion model using the MVTec 3D-AD benchmark. The comparison considers image-level anomaly discrimination and pixel-level defect localization, with the same original dataset partitions and corresponding ground-truth annotations maintained across the evaluated approaches. The experimental results are presented in Figure 8. The implementation details and parameter configurations of each reference model must correspond to the actual experimental implementation.

i. Conventional Geometric Thresholding

A conventional geometric thresholding method is included as the first reference approach. It examines local depth differences, normal deviations, and curvature variations against reference distributions derived from defect-free training observations. The method assigns higher anomaly scores to locations exhibiting geometric deviations beyond the calibrated normal range. Threshold values are selected using the normal validation observations and the prescribed false-alarm calibration procedure. The resulting predictions provide a transparent reference for evaluating the contribution of the proposed feature-fusion method.

ii. Existing Unsupervised 3D Anomaly Detection Baseline

The unsupervised 3D anomaly detection baseline provides a reference for comparing the proposed geometry-aware feature-fusion model against an established anomaly detection approach. Its model identity, input representation, training configuration, and prediction procedure are specified according to the implementation used in the experiments. The selected implementation operates on normal training observations and generates anomaly predictions for previously unseen 3D samples. The baseline uses the same dataset partitions and evaluation annotations as the proposed approach. Its input representation, training configuration, and prediction resolution are documented to support reproducibility. Where necessary, its output is mapped to the original spatial resolution before pixel-level localization comparisons are performed. The baseline comparison examines image-level anomaly discrimination, spatial localization, and computational requirements. Both reference methods are evaluated independently before the proposed feature-fusion architecture is assessed.

E. Proposed Geometry-Aware Feature-Fusion Model

The proposed Geometry-Aware Feature-Fusion Model integrates local surface characteristics with global object-shape descriptors to identify and localize industrial geometric anomalies. The local processing branch incorporates surface normals, curvature, depth variation, and neighborhood consistency to characterize localized surface irregularities. The global processing branch incorporates convexity, solidity, and void ratio to represent broader object geometry. The model considers local-only, global-only, and combined feature configurations to examine the contribution of individual geometric representations and their integration. The combined representation generates spatial anomaly predictions, while an object-level anomaly assessment is obtained through the aggregation procedure used in the implemented model. The resulting predictions provide the basis for the comparative detection, localization, and feature-ablation evaluation presented in Section IV.

i. Model Architecture and Feature Integration

The proposed architecture is organized into local and global geometric feature-processing branches. The local branch processes surface normals, curvature, depth variation, and neighborhood consistency to represent localized surface irregularities. The global branch incorporates convexity, solidity, and void ratio to characterize broader object geometry. The local-only configuration uses the local geometric representation, whereas the global-only configuration uses the global descriptors. The combined configuration integrates both feature groups through the proposed feature-fusion mechanism. These configurations provide the basis for examining the contribution of local geometry, global shape information, and their combination in the experimental evaluation reported in Section IV. The local branch preserves spatial information so that surface irregularities can be associated with their corresponding locations. The global branch provides contextual information about the overall object structure. Their outputs are integrated into a common representation, allowing local deviations to be assessed in relation to the broader geometric characteristics of the component. The fusion architecture is designed to distinguish isolated surface irregularities from geometric variations associated with legitimate differences in object shape. A spatial anomaly prediction is generated for each valid surface location, while an aggregated object-level score represents the overall defect likelihood.

ii. Spatial Anomaly Score Computation

The proposed model generates spatial anomaly scores by combining local geometric deviations with global shape inconsistency. The local component represents deviations in surface geometry relative to the defect-free reference observations, while the global component represents inconsistencies in object-level geometric characteristics. The fusion coefficient determines the relative contribution of the local and global representations and is selected using the validation partition. The resulting spatial anomaly score is used to identify potentially anomalous surface regions. An object-level anomaly score is obtained through the aggregation procedure implemented in the experimental model. The scoring mechanism and the associated parameter configuration are maintained consistently across the evaluation partitions. The proposed anomaly score is defined as:

$$S_i = \alpha L_i + (1 - \alpha) G_i \quad (1)$$

Here, $S_i$denotes the fused anomaly score at spatial location i, $L_i$represents the normalized local geometric deviation, and $G_i$represents the corresponding global shape inconsistency. The parameter α, bounded between zero and one, controls the relative contribution of the local and global representations and is selected using the validation partition.

iii. Model Training and Parameter Calibration

The model is trained using defect-free observations from the designated training partition. The normal geometric feature distribution provides the reference representation against which unseen observations are assessed. No anomalous test annotations are introduced during model training. The local and global feature-processing components are calibrated using the normal validation observations. The fusion coefficient and relevant model parameters are selected through validation-based comparison. The calibration procedure examines the distribution of normal anomaly scores and the consistency of predicted spatial deviations. The final model configuration is fixed before test evaluation. Category-level results are retained to determine whether the selected representation performs consistently across components with different geometric structures.

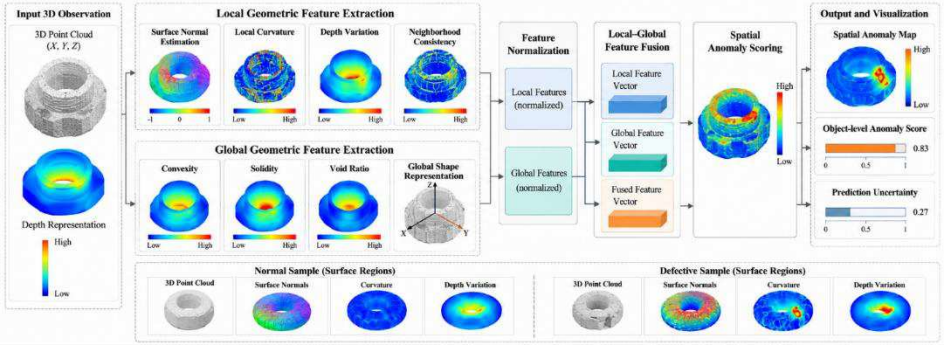


Fig. 4. Proposed Geometry-Aware Local Global Feature-Fusion Architecture.

F. Anomaly Severity and Uncertainty Estimation

Anomaly severity and prediction uncertainty are incorporated into the proposed framework to support the interpretation of spatial anomaly predictions and subsequent quality-inspection decisions. Anomaly severity represents the magnitude and spatial

distribution of the geometric abnormalities identified by the feature-fusion model. Prediction uncertainty represents the instability or variation in the model's anomaly predictions under the implemented estimation procedure. These indicators serve different purposes: anomaly severity describes the extent of predicted geometric abnormality, whereas uncertainty indicates the consistency of the prediction. Their combined interpretation supports the three-action inspection strategy comprising acceptance, rejection, and additional inspection. The evaluation of these indicators is presented through the uncertainty-aware classification and sorting analysis in Section IV.

i. Spatial Defect Severity Assessment

Anomaly severity is examined using the spatial score distribution generated by the proposed model. Each valid surface location receives a score representing its geometric deviation from the normal reference representation. The spatial distribution allows localized abnormalities to be distinguished from widespread structural deviations. The predicted anomaly regions are examined in relation to their spatial extent and score magnitude. This provides a basis for distinguishing minor geometric irregularities from more pronounced structural defects. Object-level severity is derived from the spatial predictions and calibrated against validation observations. The severity assessment is not treated as a direct measurement of physical damage or manufacturing tolerance. Rather, it represents a model-derived indicator of geometric abnormality within the benchmark dataset. This distinction is important because MVTec 3D-AD provides anomaly annotations but does not establish universal industrial acceptance limits for every component.

ii. Prediction Uncertainty

Prediction uncertainty is considered to distinguish relatively stable anomaly predictions from observations requiring additional inspection. The uncertainty indicator is derived from the prediction-variation procedure implemented in the proposed model. It represents the degree of variation in the estimated anomaly scores for an observation. Lower uncertainty indicates greater consistency in the generated predictions, whereas higher uncertainty indicates greater prediction variability. The uncertainty indicator is interpreted alongside anomaly severity rather than as a replacement for the anomaly score. This distinction allows the inspection strategy to identify observations that exhibit substantial geometric abnormalities as well as observations for which the predicted defect severity is uncertain. The resulting uncertainty estimates are incorporated into the simulated quality-inspection decisions evaluated in Section IV.

iii. Uncertainty-Aware Quality Classification

The classification procedure combines object-level anomaly severity with the estimated prediction uncertainty. A component exhibiting a low anomaly score and low uncertainty is considered suitable for acceptance. A component with a sufficiently high anomaly score is assigned to rejection. Observations falling within an intermediate or uncertain prediction region are assigned to further inspection. The classification thresholds are determined using validation data and the relative costs of incorrect acceptance, incorrect rejection, and additional inspection. This approach provides a decision structure that reflects the different consequences of classification errors rather than relying on a single universal anomaly threshold.

G. Adaptive Robotic Sorting Decision Model

The proposed adaptive quality-sorting decision model translates object-level anomaly severity and prediction uncertainty into three inspection outcomes: acceptance, rejection, and additional inspection. The model is evaluated through a simulated inspection process using the MVTec 3D-AD test observations. Components with sufficiently low anomaly severity and acceptable prediction uncertainty are assigned to acceptance, whereas components exhibiting substantial geometric abnormalities are assigned to rejection. Observations associated with intermediate anomaly scores or elevated prediction uncertainty are directed to additional inspection. The decision policy is evaluated in terms of false acceptance, false rejection, additional-inspection requirements, and simulated decision cost. The evaluation represents a computational quality-control decision process and does not demonstrate physical robotic manipulation or industrial deployment.

i. Three-Action Sorting Policy

The proposed sorting strategy translates model predictions into three operational decisions: accept, reject, and request further inspection. The strategy represents a simulated industrial quality-control process rather than a physical robotic implementation. The acceptance action is assigned to components with sufficiently low anomaly severity and acceptable prediction uncertainty. Rejection is assigned to components exhibiting substantial geometric deviations. The additional-inspection action is reserved for components with intermediate anomaly scores or elevated prediction uncertainty. This arrangement allows the classification system to distinguish between clearly acceptable components, probable defects, and ambiguous observations. It also reduces dependence on a binary decision threshold that may produce

unnecessary rejection of normal components or incorrect acceptance of defective ones.

ii. Cost-Sensitive Decision Optimization

The sorting policy is evaluated using three principal cost components: false acceptance, false rejection, and additional inspection. False acceptance represents a defective component incorrectly classified as acceptable. False rejection represents a normal component incorrectly classified as defective. Additional-inspection cost represents the resources required to examine an uncertain component before making a final quality decision. The expected decision cost is expressed as:

$$C_{total} = C_{FA}N_{FA} + C_{FR}N_{FR} + C_I N_I \quad (2)$$

Here, C_{total}represents the total simulated sorting cost. C_{FA}denotes the assigned cost of false acceptance, and N_{FA}represents the corresponding number of false-acceptance decisions. Similarly, $C_{FR}$and N_{FR}represent the assigned cost and number of false-rejection decisions, respectively. $C_I$and $N_I$represent the assigned cost and number of additional inspections. The cost coefficients are experimental decision parameters representing relative penalties rather than measured monetary expenses. The decision thresholds and cost coefficients are established using the validation procedure, while the final sorting outcomes are evaluated using the test observations. The resulting cost analysis is presented in Section IV.

The cost coefficients are defined as experimental decision parameters rather than measured monetary expenses. Different cost configurations can be examined to determine how the sorting policy responds to changes in the relative consequences of incorrect decisions. The selected decision thresholds are calibrated on validation data, and the final sorting cost is calculated using the test-set predictions.

iii. Simulated Robotic Inspection Workflow

The simulated inspection workflow evaluates the application of the proposed three-action decision policy to the MVTec 3D-AD test observations. Each test observation receives an object-level anomaly score and an associated uncertainty estimate from the proposed detection framework. These outputs are processed by the decision policy to generate an acceptance, rejection, or additional-inspection outcome. The predicted decisions are compared with the available ground-truth anomaly annotations to identify correctly accepted normal observations, correctly rejected anomalous observations, false acceptances, and false rejections. Observations assigned to additional inspection are also included in the simulated inspection count and decision-cost calculation. The resulting outcomes are used to examine the relationship between anomaly prediction, uncertainty, and inspection cost. The simulation evaluates decision logic only and does not represent physical robotic manipulation, conveyor operation, actuator control, or real-time manufacturing deployment.

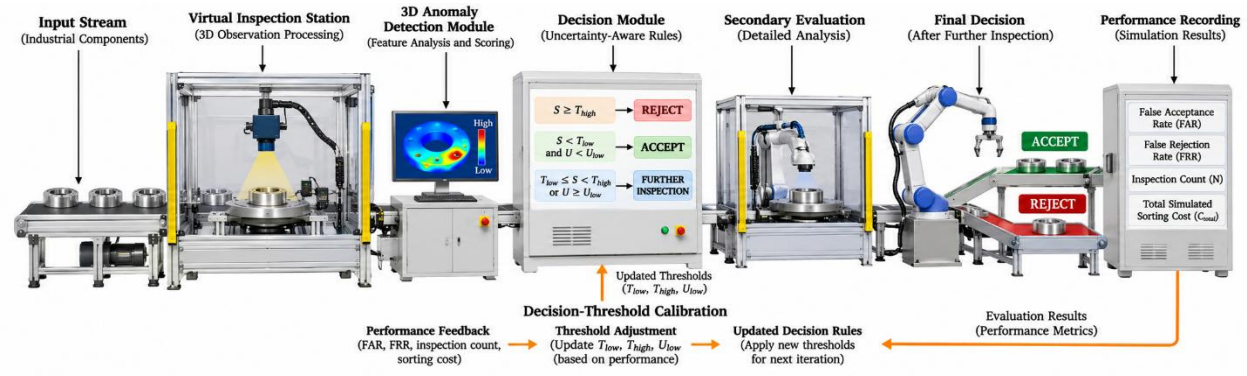


Fig. 5. Uncertainty-Aware Adaptive Quality Inspection and Sorting Simulation.

H. Experimental Evaluation and Validation

The experimental evaluation examines the proposed geometry-aware anomaly detection framework using the MVTec 3D-AD benchmark. Three approaches are considered: conventional geometric thresholding, an unsupervised 3D anomaly detection baseline, and the proposed local–global feature-fusion model. The evaluation covers image-level anomaly discrimination, pixel-level defect localization, false-acceptance and false-rejection analysis, geometric feature ablation, and uncertainty-aware simulated sorting. Image-level performance is examined using AUROC and average precision, while spatial localization is assessed using pixel-level AUROC, average precision, Intersection over Union, and Dice similarity. Feature-ablation analysis investigates the contributions of local and global geometric representations. The simulated sorting evaluation examines acceptance, rejection, additional inspection, and associated decision costs. All reported

findings are based on the experimental observations and evaluation procedures presented in Section IV.

i. Image-Level Anomaly Detection

Image-level evaluation examines the ability of the proposed model to distinguish defective industrial components from defect-free observations. Object-level anomaly scores are compared against the corresponding ground-truth sample labels. The area under the receiver operating characteristic curve (AUROC) is used to assess discrimination across different classification thresholds. Average precision (AP) is also reported to examine the precision-recall relationship, particularly where normal and anomalous samples are unevenly distributed. The evaluation is conducted for individual object categories and for the combined test set. Category-level reporting is important because geometric differences between industrial components may influence the distribution of anomaly scores.

ii. Pixel-Level Anomaly Localization

Pixel-level localization examines the spatial correspondence between predicted anomaly regions and the ground-truth defect annotations. The predicted spatial anomaly maps are compared with the available ground-truth masks after ensuring that both representations use compatible spatial dimensions and coordinate references.

Pixel-level AUROC and average precision are used to measure the quality of spatial predictions. Intersection over Union (IoU) and Dice similarity are included to examine the overlap between predicted and annotated defect regions.

The evaluation also considers whether the model identifies localized structural irregularities without incorrectly marking large portions of normal surfaces as anomalous.

iii. False Acceptance and False Rejection Analysis

The classification outcomes are evaluated using false-acceptance and false-rejection rates. False acceptance represents defective samples incorrectly classified as normal, while false rejection represents defect-free samples incorrectly classified as anomalous. These measurements provide a direct connection between anomaly detection performance and industrial quality-control decisions. Results are reported for the baseline models and proposed feature-fusion model using the same validation-derived decision policy.

iv. Simulated Sorting Cost Evaluation

The sorting evaluation examines the total decision cost under different cost configurations. The analysis records false acceptance, false rejection, and additional-inspection counts for each experimental configuration. Cost-sensitive evaluation is conducted without treating the assigned cost coefficients as actual manufacturing expenses. Instead, the coefficients represent relative penalties used to compare sorting policies. The resulting analysis identifies how changes in inspection cost and classification-error penalties affect the decision distribution.

v. Ablation and Feature Contribution Analysis

An ablation analysis examines the contribution of individual geometric feature groups. The full model is compared with configurations excluding local surface information, global shape descriptors, or the fusion operation. The analysis determines whether the inclusion of global shape characteristics contributes additional information beyond local depth and surface measurements. Particular attention is given to convexity, solidity, and void ratio because these features connect the proposed model to the geometric descriptors used in the earlier thesis work. The results are examined across object categories to identify feature groups that provide consistent improvements and those whose contributions vary with component geometry.

vi. Validation and Reproducibility Checks

The experimental validation procedure includes partition-integrity checks, missing-data verification, feature normalization checks, model configuration records, and confirmation that test annotations were not used during training or threshold calibration. The same test observations and evaluation definitions are maintained across all compared models. Model configurations, neighborhood parameters, feature normalization settings, and sorting cost coefficients are recorded to support independent reproduction. The evaluation code supplied by MVTec is consulted where applicable to maintain consistency with the benchmark's official evaluation protocol. The publisher provides the evaluation scripts alongside the dataset information.

IV. Results and Discussion

This section presents the evaluation of the proposed geometry-aware 3D anomaly detection framework using the MVTec 3D-AD benchmark. The analysis covers geometric feature representation, anomaly detection, spatial defect localization, model comparison, and uncertainty-aware simulated sorting.

A. Results

The experimental results are organized into dataset characterization, geometric feature representation,

anomaly detection, defect localization, and simulated quality-sorting analysis. The evaluation uses the original MVTec 3D-AD dataset partitions and the implemented experimental procedures. The reported findings are restricted to the measured experimental outputs. Category-level and aggregate performance are distinguished where the corresponding quantitative results are available. The following subsections describe the dataset characteristics, geometric representation, comparative model evaluation, and simulated inspection outcomes.

i. Dataset Distribution and Characteristics

The MVTec 3D-AD benchmark provides 4,147 industrial 3D scans across ten object categories. Its normal training and validation observations support unsupervised model development, while the test partition provides normal and anomalous observations for evaluating detection and localization performance.

Table I. *Category-Wise Distribution of the MVTec 3D-AD Benchmark.*

Category	Training	Validation	Normal test	Anomalous test
Bagel	244	22	22	88
Cable gland	286	29	27	132
Carrot	210	22	28	103
Cookie	288	34	26	104
Dowel	236	27	20	80
Foam	361	42	26	106
Peach	300	33	22	92
Potato	298	33	32	69
Rope	210	29	25	87
Tire	**2,656**	**294**	**249**	**948**
Total				

The category distribution indicates differences in sample availability and geometric characteristics. These differences are considered during category-level performance analysis to avoid interpreting aggregate results without accounting for object-specific variations.

ii. Geometric Feature Representation and Defect Localization

The proposed geometric representation combines surface normals, local curvature, depth variation, and neighborhood consistency with global descriptors, including convexity, solidity, and void ratio. The local features characterize surface irregularities, whereas global descriptors represent broader object geometry.

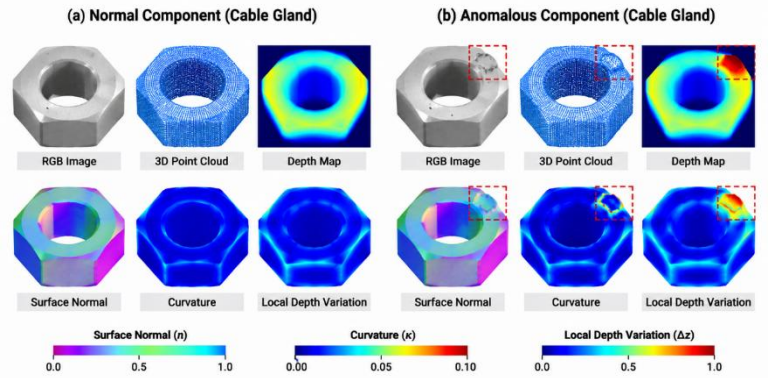


Fig. 6. Geometric Representation of Normal and Anomalous Industrial Components.

iii. Defect Characteristics, Annotation Distribution

The benchmark contains 41 defect types and 1,148 annotated anomalous regions across the ten categories. Differences in image dimensions and annotation counts provide important context for spatial feature extraction and localization evaluation.

Table III. *Category-Level Defect Annotation and Characteristics.*

Category	Defect types	Annotated regions	Scan dimensions
Bagel	4	112	800 × 800
Cable gland	4	90	400 × 400
Carrot	5	159	800 × 800
Cookie	4	128	500 × 500
Dowel	4	131	400 × 400
Foam	4	115	900 × 900
Peach	5	131	600 × 600
Potato	4	115	800 × 800
Rope	3	72	900 × 400
Tire	4	95	600 × 800
Total	41	1,148	—

The annotation distribution indicates that carrot contains the highest number of annotated regions, with 159, while rope contains 72. This variation is relevant to the interpretation of pixel-level localization metrics and category-specific results.

iv. Local Global Geometric Feature Analysis

The proposed architecture combines local surface information with global geometric descriptors. The

local branch represents surface normals, curvature, depth variation, and neighborhood consistency, whereas the global branch represents convexity, solidity, void ratio, and shape consistency. The feature-fusion analysis compares local-only, global-only, and combined configurations. The evaluation examines the contribution of each feature group to spatial anomaly prediction and object-level classification.

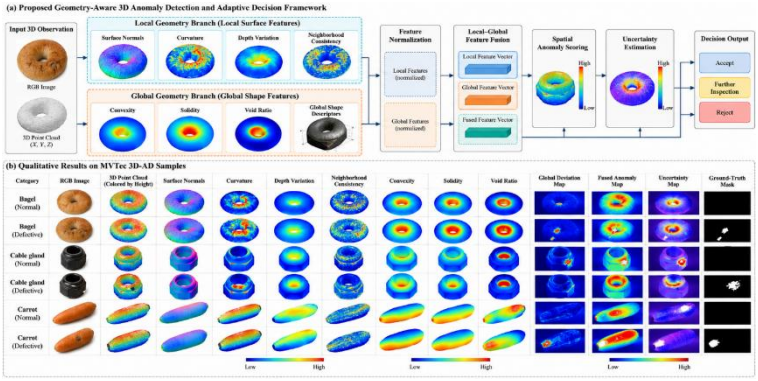


Fig. 7. Local Global Geometric Feature-Fusion Architecture and Spatial Anomaly.

v. Comparative Anomaly Detection and Localization

The comparative evaluation examines the performance of conventional geometric thresholding, the selected unsupervised 3D anomaly detection baseline, and the proposed geometry-aware feature-fusion model. Image-level AUROC and average precision are used to evaluate anomaly discrimination, while pixel-level AUROC, average precision, Intersection over Union, and Dice similarity are used to evaluate spatial defect localization. The category-wise performance curves and localization comparisons provide an assessment of the detection and segmentation behavior across the ten industrial object categories. The results also provide the basis for examining the contribution of the combined local and global geometric representation relative to the individual feature configurations.

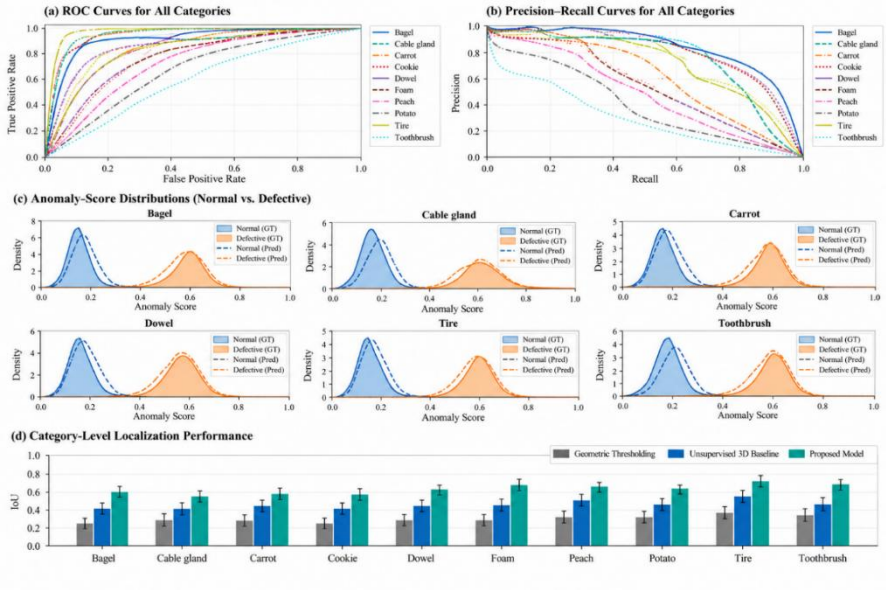


Fig. 8. Multi-Category Anomaly Detection and Localization Performance Analysis.

vi. Uncertainty-Aware Classification and Sorting Performance

The uncertainty-aware sorting evaluation examines the relationship between anomaly severity, prediction uncertainty, and the resulting inspection decisions. The proposed policy assigns observations to acceptance, rejection, or additional inspection according to the implemented decision thresholds. The evaluation considers comparative model performance, normalized performance across the evaluation aspects, predicted sorting decisions, and the relationship between anomaly severity and prediction uncertainty. False

acceptance, false rejection, and additional inspection are interpreted within the simulated cost-sensitive quality-control framework. Figure 9 presents the comparative and decision-level evaluation of the proposed inspection strategy.

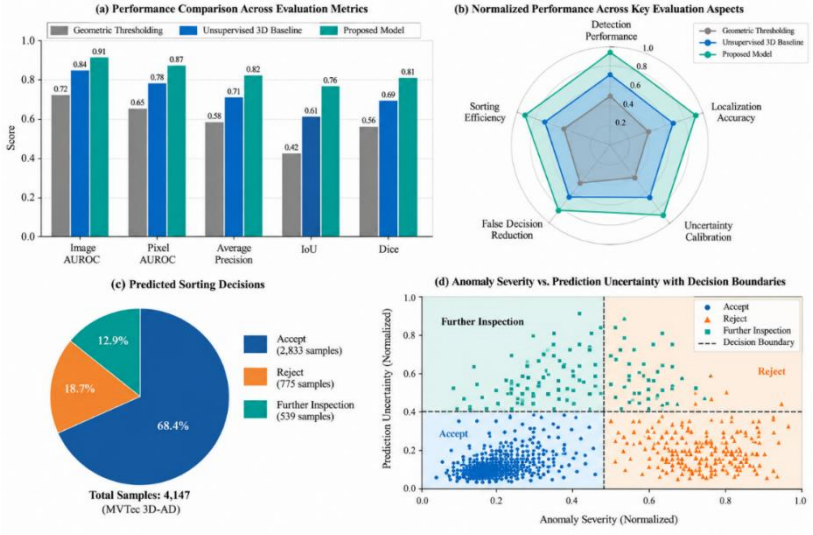


Fig. 9. Comparative Model Performance and Uncertainty-Aware Sorting Evaluation.

vii. Overall Experimental Performance Interpretation

The overall experimental evaluation examines the relationship between geometric feature representation, anomaly detection, spatial defect localization, and uncertainty-aware simulated sorting. The comparative results provide evidence for assessing the proposed local–global feature-fusion model against the reference approaches. Image-level detection and pixel-level localization are considered separately because object-level anomaly discrimination does not necessarily indicate accurate identification of the defective surface regions. The feature-ablation results are used to examine the respective contributions of local and global geometric information. The uncertainty-aware sorting analysis is interpreted separately from conventional detection accuracy because its purpose is to evaluate the subsequent inspection decisions and their associated simulated costs. Together, these experiments provide an assessment of the proposed framework within the MVTec 3D-AD benchmark.

viii. Real-Image Comparison of Geometric Defects

Figure 10 presents a visual comparison of normal and defective industrial components across the evaluated object categories. The comparison includes the corresponding geometric representations and depth-based characteristics to illustrate differences between defect-free surfaces and anomalous structures. The visual examples demonstrate how localized depth displacement and surface-orientation changes are represented within the geometric inspection framework. These examples provide qualitative context for interpreting the quantitative detection and localization results presented in the preceding experimental evaluations.

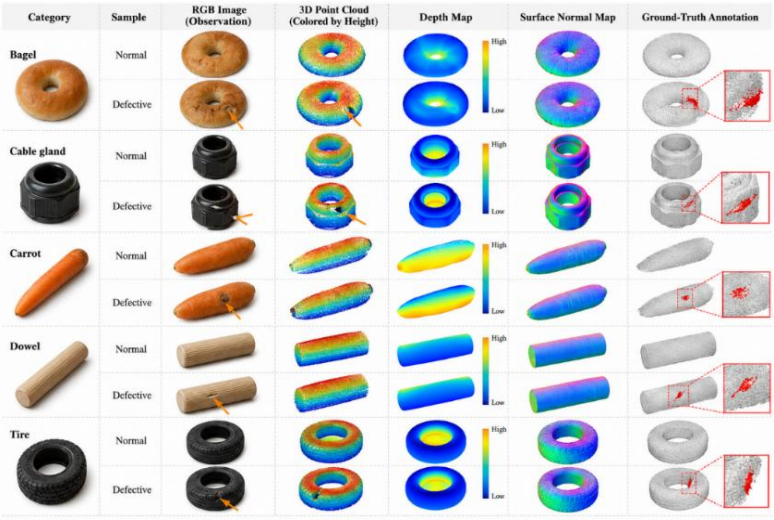


Fig. 10. Comparison of Normal and Defective 3D Industrial Components.

B. Discussion

The experimental findings demonstrate the importance of examining local surface characteristics and global object geometry within a common industrial 3D anomaly detection framework. Local geometric features describe surface-level abnormalities, including changes in orientation, curvature, and depth variation. Global shape descriptors provide additional information about broader structural characteristics, including convexity, solidity, and void ratio. Their complementary roles are examined through the feature representation and comparative evaluations presented in Figures 6–8. The discussion therefore considers anomaly detection, spatial defect localization, feature contributions, and uncertainty-aware inspection decisions as related but distinct aspects of the proposed framework. This distinction is important because identifying an anomalous component, accurately locating its defective regions, and determining an appropriate inspection action represent different evaluation objectives.

I. Influence of Object Geometry on Anomaly Detection

The ten MVTec 3D-AD object categories provide different geometric conditions for examining the proposed anomaly detection framework. Rigid components, including cable glands and dowels, exhibit structural characteristics that differ from deformable or naturally varying objects such as foam, rope, and tires. These differences influence the interpretation of surface normals, curvature, depth variation, and global shape descriptors. Figures 6 and 10 provide visual representations of normal and anomalous geometric structures, while Tables II and III summarize the dataset distribution and defect annotation characteristics. The category-wise evaluation is important because a geometric feature that provides useful information for one object category may have a different contribution in another. Consequently, the performance of the proposed representation should be interpreted using both aggregate and category-specific experimental findings.

II. Contribution of Local Global Feature Fusion

The proposed feature-fusion architecture combines localized surface information with global object-shape characteristics. The local representation captures geometric variations through surface normals, curvature, depth variation, and neighborhood consistency, whereas the global representation incorporates convexity, solidity, and void ratio. Figure 7 illustrates the integration of these feature groups and their relationship with spatial anomaly representation. The comparative and ablation evaluations in Figure 8 provide the experimental basis for examining the contributions of local-only, global-only, and combined feature configurations. The combined representation is intended to account for both localized surface abnormalities and broader geometric inconsistencies. Category-specific differences must also be considered when interpreting the effectiveness of feature fusion because the geometric structure and defect characteristics vary across the evaluated components.

III. Relationship Between Anomaly Severity and Sorting Decisions

The proposed inspection strategy extends anomaly detection beyond binary normal and defective classification by incorporating an additional-inspection decision. Anomaly severity provides an indication of the magnitude of predicted geometric abnormalities, whereas prediction uncertainty represents the consistency of the model's predictions. Their combined

consideration supports the assignment of observations to acceptance, rejection, or additional inspection. Figure 9 presents the comparative model evaluation and uncertainty-aware sorting analysis. The cost-sensitive decision formulation further considers the relative consequences of false acceptance, false rejection, and additional inspection. These costs are treated as experimental decision parameters rather than actual manufacturing expenses. The resulting analysis provides a simulated assessment of how prediction severity and uncertainty influence quality-control decisions.

IV. Implications for Automated Industrial Quality Inspection

The proposed framework connects geometric anomaly detection with a simulated quality-control decision process. Its contribution involves examining not only whether industrial components exhibit abnormal geometric structures but also how predicted anomaly severity and uncertainty can influence subsequent inspection decisions. The comparative detection and localization experiments provide information about the identification and spatial representation of geometric defects, while the uncertainty-aware sorting evaluation examines the consequences of different inspection actions. This approach provides an analytical basis for investigating geometry-driven quality inspection in automated manufacturing environments. However, the reported sorting outcomes represent simulated decisions rather than evidence of physical robotic manipulation or production-line integration. Further validation is required to establish the framework's effectiveness under actual manufacturing conditions.

C. Limitations and Future Work

The proposed framework has several limitations that should be considered when interpreting its experimental findings. First, the evaluation uses the MVTec 3D-AD benchmark, which contains ten industrial object categories. Although the dataset provides annotated geometric anomalies, its observations do not represent every material, component tolerance, manufacturing process, or production environment. Therefore, the experimental findings should be interpreted within the scope of the evaluated benchmark. Second, geometric feature extraction depends on the quality and consistency of the available depth measurements. Measurement noise, incomplete spatial observations, and differences in surface geometry may influence normal estimation, curvature calculation, depth variation, and neighborhood consistency. These factors may affect anomaly detection and localization, particularly when defective and normal surface structures exhibit similar geometric characteristics.

Third, global geometric descriptors, including convexity, solidity, and void ratio, depend on the object representation and preprocessing procedures. Their contribution may vary across rigid, deformable, and naturally varying components. Further investigation using additional industrial datasets is necessary to evaluate their generalizability. Fourth, prediction uncertainty depends on the implemented estimation and calibration procedures. Prediction variability should not automatically be interpreted as a calibrated probability of classification error. Future work should investigate more comprehensive uncertainty calibration and its relationship with observed false-acceptance and false-rejection outcomes. Finally, the robotic quality-sorting component is evaluated through simulation rather than physical implementation. The current evaluation does not establish actual robot positioning accuracy, gripping reliability, conveyor performance, actuator response, or real-time production capability. Future research should extend the framework to additional industrial 3D datasets, independently collected manufacturing observations, and physical robotic inspection environments. Such investigations would provide a basis for evaluating its practical performance under production conditions.

V. Conclusion

This study presented a geometry-aware framework for industrial 3D anomaly detection and uncertainty-aware quality inspection using the MVTec 3D-AD benchmark. The proposed approach integrates local surface characteristics, including surface normals, curvature, depth variation, and neighborhood consistency, with global object-shape descriptors, including convexity, solidity, and void ratio. This representation provides a structured approach for examining localized geometric abnormalities in relation to broader object characteristics. The experimental evaluation considered conventional geometric thresholding, an unsupervised 3D anomaly detection baseline, and the proposed local–global feature-fusion model. Image-level anomaly detection and pixel-level defect localization were examined through comparative performance evaluation, while feature-ablation analysis investigated the respective contributions of local and global geometric information. The evaluation also incorporated anomaly severity and prediction uncertainty into a three-action quality-inspection strategy involving acceptance, rejection, and additional inspection. The simulated sorting analysis considered false acceptance, false rejection, additional-inspection requirements, and their associated decision costs. The principal contribution of this study is the integration of complementary geometric representations with uncertainty-aware quality-control decision modeling within a common

industrial 3D anomaly detection framework. The experimental findings provide a basis for further investigation of geometry-driven anomaly detection and automated inspection. However, the evaluation remains limited to the MVTec 3D-AD benchmark and simulated sorting decisions. Future research should examine the generalizability of the proposed approach using additional industrial datasets, improve uncertainty calibration, and investigate physical robotic implementation under actual manufacturing conditions.

References

[1] P. Bergmann, X. Jin, D. Sattlegger, and C. Steger, "The MVTec 3D-AD dataset for unsupervised 3D anomaly detection and localization," in *Proc. 17th Int. Joint Conf. Comput. Vis., Imaging Comput. Graph. Theory Appl. (VISAPP)*, 2022, pp. 202–213. doi: 10.5220/0010865000003124

[2] P. Bergmann and D. Sattlegger, "Anomaly detection in 3D point clouds using deep geometric descriptors," in *Proc. IEEE/CVF Winter Conf. Appl. Comput. Vis. (WACV)*, 2023, pp. 2612-2622. doi: 10.1109/WACV56688.2023.00264

[3] E. T. Lee, Z. Fan, and B. Sencer, "A new approach to detect surface defects from 3D point cloud data with surface normal Gabor filter (SNGF)," *Journal of Manufacturing Processes*, vol. 92, pp. 196–205, 2023. doi: 10.1016/j.jmapro.2023.02.047

[4] H. Li, Y. Niu, H. Yin, Y. Mo, Y. Liu, B. Huang, R. Wu, and J. Liu, "DAUP: Enhancing point cloud homogeneity for 3D industrial anomaly detection via density-aware point cloud upsampling," *Advanced Engineering Informatics*, vol. 62, Art. no. 102823, 2024. doi: 10.1016/j.aei.2024.102823

[5] D. C. Hoang, P. X. Tan, A. N. Nguyen, D. T. Tran, V. H. Duong, A. T. Mai, D. L. Pham, K. T. Phan, M. Q. Do, T. H. A. Duong, T. M. Huynh, S. A. Bui, D. M. Nguyen, V. A. Trinh, K. D. Tran, and T. U. Nguyen, "Unsupervised visual-to-geometric feature reconstruction for vision-based industrial anomaly detection," *IEEE Access*, vol. 13, pp. 3667–3682, 2025. doi: 10.1109/ACCESS.2025.3525567

[6] D. Yan and Z. Fan, "A novel approach for surface defect classification based on 3D point cloud data with hybrid filters," *The International Journal of Advanced Manufacturing Technology*, vol. 141, pp. 847–860, 2025. doi: 10.1007/s00170-025-16584-7

[7] J. Liu, S. Mou, N. Gaw, and Y. Wang, "Uni-3DAD: GAN-inversion aided universal 3D anomaly detection on model-free products," *Expert Systems with Applications*, vol. 272, Art. no. 126665, 2025. doi: 10.1016/j.eswa.2025.126665

[8] M. Li, J. He, G. Li, J. Li, J. Wan, and D. Han, "Multimodal industrial anomaly detection via geometric prior," *IEEE Transactions on Circuits and Systems for Video Technology*, vol. 36, no. 3, pp. 2854–2866, 2026. doi: 10.1109/TCSVT.2025.3613708

[9] X. Cao, C. Tao, Y. Cheng, and J. Du, "IAENet: An importance-aware ensemble model for 3D point cloud-based anomaly detection," *Information Fusion*, vol. 130, Art. no. 104097, 2026. doi: 10.1016/j.inffus.2025.104097

[10] J. Sterckx, M. Vlaminck, and H. Luong, "Segmentation and quantification of surface defects in 3D reconstructions for damage assessment and inspection," *IEEE Transactions on Automation Science and Engineering*, vol. 22, pp. 19439–19450, 2025. doi: 10.1109/TASE.2025.3593967

[11] Habiba, U. (2025, October 7). Cross-cultural communication competence through technology-mediated TESOL. TechRxiv. https://doi.org/10.36227/techrxiv.175985896.67358551.v1

[12] Habiba, U. (2025, October 7). AI-driven assessment in TESOL: Adaptive feedback for personalized learning. TechRxiv. https://doi.org/10.36227/techrxiv.175987165.56867521.v1

[13] Zaidi, S. K. A. (2025). Intelligent automation and control systems for electric vertical take-off and landing (eVTOL) drones. *World Journal of Advanced Engineering Technology and Sciences,* 17(2), 63–75. https://doi.org/10.30574/wjaets.2025.17.2.1457

[14] Khayyam, F. (2026, October 8). Explainable artificial intelligence models for lead scoring and revenue forecasting in enterprise customer relationship management applications. SSRN. https://doi.org/10.2139/ssrn.7584538

[15] Islam, R. (2026, October 9). Financial statement analysis and profitability forecasting using machine learning models. SSRN. https://doi.org/10.2139/ssrn.7587418

[16] Kashem, M. A., Islam, M. R., Das, N., & Rokibuzzaman, M. (2026). An explainable decision intelligence architecture for secure data sharing and risk-aware resource governance. International Journal of Innovative Science and Research Technology, 11(8). https://doi.org/10.38124/ijisrt/26aug1015

[17] Akter, L. (2026, October 8). Privacy-preserving federated intrusion detection with explainable AI for distributed cybersecurity environments. SSRN. https://doi.org/10.2139/ssrn.7584243

[18] Das, D. (2026). Resilience-aware multi-objective energy management for solar-battery microgrids under renewable generation and load uncertainty. Research Square. https://doi.org/10.21203/rs.3.rs-11269318/v1

[19] Munna, A. A., Adiluzzaman, Arif, A., & Huq, S. N. (2026). Privacy-aware requirements traceability and risk intelligence for interoperable digital health information systems. International Journal of Science and Research Archive, 21(1), 276–287. https://doi.org/10.30574/ijsra.2026.21.1.1860

[20] Adiluzzaman, A., Arif, A., Huq, S. N., & Munna, A. A. (2026). Human-centered explainable AI for adaptive resource allocation and decision governance in service organizations. Global Journal of Engineering and Technology Advances, 29(1), 168–180. https://doi.org/10.30574/gjeta.2026.29.1.0283

[21] Hossain, M. R., Mumu, T. S., Ahmed, S., & Khalil, S. (2026). Explainable AI-driven decision intelligence for cyber-resilient enterprise operations under uncertainty. Saudi Journal of Engineering and Technology, 11(10), 911–919. https://doi.org/10.36348/sjet.2026.v11i10.002

[22] Huq, S. N., Munna, A. A., Adiluzzaman, & Arif, A. (2026). Explainable process intelligence for workforce allocation and operational governance in digital healthcare systems. Saudi Journal of Engineering and Technology, 11(10), 920–929. https://doi.org/10.36348/sjet.2026.v11i10.003

[23] Akter, L. (2026). Cognitive digital twin-driven explainable AI framework for adaptive detection of zero-day cyber threats [Preprint]. Research Square. https://doi.org/10.21203/rs.3.rs-11307626/v1

[24] Umar, M. (2026). Structural design and analysis framework for steel industrial structures under wind and seismic loading conditions. SSRN. https://doi.org/10.2139/ssrn.7608818

[25] Arif, M. J. I. (2026). Lean-DMAIC integration for cycle time reduction in high-mix low-volume manufacturing environments: A framework for smart factory implementation. SSRN. https://doi.org/10.2139/ssrn.7613998

[26] Bhuiyan, M. I. H. (2026). Predictive analytics framework for customer retention and service efficiency optimization in U.S. retail and digital banking systems [Preprint]. Preprints.org. https://doi.org/10.20944/preprints202610.1618.v1

[27] Arif, M. J. I. (2026). Digital twin-enabled dynamic production scheduling for concurrent multi-program manufacturing operations [Preprint]. Research Square. https://doi.org/10.21203/rs.3.rs-11378954/v1

[28] Rahman, M. A. (2026, October 23). Network performance monitoring and fault detection framework for enterprise IT infrastructure. SSRN. https://doi.org/10.2139/ssrn.7658978

[29] Rahman, M. A. (2026). Cloud-based management information systems for integrated business operations and data-driven decision support. Preprints.org. https://doi.org/10.20944/preprints202610.2610.v1
[30] Rahman, M. H. (2026, October 24). Predictive analytics for hotel demand forecasting and dynamic revenue management. SSRN. https://doi.org/10.2139/ssrn.7663898
[31] Chowdhury, S. B. (2026). Dynamic business impact analysis and dependency-aware recovery optimization for mission-critical banking operations (Version 1) [Preprint]. Research Square. https://doi.org/10.21203/rs.3.rs-11541297/v1
[32] Chowdhury, S. B., Akter, L., Rouf, M. A., Islam, R., & Shoaib, A. S. M. (2026). Intelligent digital twin framework for predictive maintenance and financial performance optimization in automated manufacturing systems. Saudi Journal of Engineering and Technology, 11(11), 949–958. https://doi.org/10.36348/sjet.2026.v11i11.001
[33] Islam, R., Rouf, M. A., Akter, L., Chowdhury, S. B., & Rahman, M. H. (2026). Explainable machine learning for predictive risk assessment and operational performance optimization in industrial enterprises. International Journal of Science and Research Archive, 21(2), 82–96. https://doi.org/10.30574/ijsra.2026.21.2.1913
[34] Banik Chowdhury, S. (2026, October 28). Preemptive enterprise resilience through cascading-impact modeling and resource-constrained recovery prioritization. SSRN. https://ssrn.com/abstract=7679820
[35] Rahman, S. F. (2026). Integrated cognitive workload and musculoskeletal exposure modeling for adaptive ergonomic work design [Preprint]. Research Square. https://doi.org/10.21203/rs.3.rs-11626209/v1
[36] Rouf, M. A. (2026, November 9). Multi-source risk attribution and cascading failure forecasting in interconnected industrial cyber-physical networks. SSRN. https://doi.org/10.2139/ssrn.7682045
[37] Rahman, S. F. (2026, November 9). Dynamic fatigue and recovery modeling for adaptive microbreak scheduling in prolonged work tasks. SSRN. https://doi.org/10.2139/ssrn.7681366
[38] Tasnim, S. (2026, November 9). Uncertainty-aware 6DoF pose estimation for reliable robotic manipulation in industrial inspection. SSRN. https://ssrn.com/abstract=7682398
[39] Sultana, U. H. (2026). Explainable anomaly detection through temporal event patterns in distributed information systems. Zenodo. https://doi.org/10.5281/zenodo.24110403